

Torque-Generating Units of the Bacterial Flagellar Motor Step Independently

Aravinthan D. T. Samuel and Howard C. Berg

Rowland Institute for Science, Cambridge, Massachusetts 02142, and Department of Molecular and Cellular Biology, Harvard University, Cambridge Massachusetts 02138 USA

ABSTRACT Measurements of the variance in rotation period of tethered cells as a function of mean rotation rate have shown that the flagellar motor of *Escherichia coli* is a stepping motor. Here, by measurement of the variance in rotation period as a function of the number of active torque-generating units, it is shown that each unit steps independently.

INTRODUCTION

A bacterial flagellum is driven at its base by a rotary motor (Berg and Anderson, 1973). It has long seemed likely that this motor steps, i.e., that the relative motion between rotor and stator is ratchetlike, marked by sudden advances or retreats, separated by waiting times during which large displacements are not allowed (Berg, 1976). However, such steps have not been observed directly. Elasticity in the elements that link torque-generating units to the cell wall or to the flagellar filament tends to smooth out discontinuities that, in any event, are obscured by Brownian movement.

Nevertheless, it is possible to measure the variance in rotation rate (or period), which reflects both the number of steps per revolution and the probability distribution of waiting times between steps (Berg et al., 1982). The easiest way of doing this is to follow the rotation of the body of a cell tethered to glass by a single flagellar filament (Silverman and Simon, 1974). Augmenting motor torque by means of electrorotation and measuring this variance as a function of mean rotation rate, we found that the behavior of the motor matches that of a stochastic stepper (Samuel and Berg, 1995). The number of steps per revolution (inversely proportional to the variance in rotation period) for a Poisson stepper (i.e., a stochastic stepper in which waiting times between steps are exponentially distributed) was estimated to be at least 400. If the waiting time for one step is not independent of that of the preceding step, this is an overestimate (cf. Svoboda et al., 1994; Schnitzer and Block, 1996).

The flagellar motor is driven by a set of discrete torque-generating units, which in *E. coli* can number as many as 8 (Blair and Berg, 1988) or 16 (Block and Berg, 1984). This can be shown by synthesis of wild-type MotA or MotB in paralyzed mutants (as in the research just cited), by reactivation with membrane potential following de-energization (Fung and Berg, 1995), or by mechanical damage and repair

(Berry et al., 1995). As the motor driving a tethered cell acquires active torque-generating units, the mean rotation rate of the cell increases, passing through a series of equally spaced levels. The simplest assumption is that different units step independently. In this case, the estimate of the number of steps per revolution based on variance will be proportional to the mean rotation rate (to level number). However, it also is possible that steps are correlated. In the extreme case, i.e., of synchronous stepping, the estimate of step number will be constant.

We synthesized wild-type MotA in cells carrying a *motA* mutation (as in Blair and Berg, 1988). We began by using cells that were wild-type for chemotaxis (strain HCB1254). In these cells, motors functioning with a single torque-generating unit rarely change direction, so it is easy to collect enough data for variance analysis. However, as the number of torque-generating units increases, switching becomes problematic. Therefore, we constructed a strain missing the chemotactic signaling component CheY that runs its motors exclusively counterclockwise (strain HCB1259). We confined our analysis to cells that exhibited at least three discrete levels of torque, so that the number of active torque-generating units could be inferred unambiguously. The number of steps per revolution taken by flagellar motors, estimated from the analysis of variance, was proportional to the number of active torque-generating units. We conclude that different torque-generating units step independently.

MATERIALS AND METHODS

Cells and tethering

Strain HCB1254 (Table 1) lacks flagellar filaments and has paralyzed motors. In the presence of isopropyl β -D-thiogalactopyranoside (IPTG, an inducer for *plac*), wild-type MotA is produced and the motors are repaired. This strain was constructed as follows:

Step 1: The Δ *flhC* mutation was transduced from JA11 into MS5037.

Step 2: The resultant transductant was transformed with pDFB36.

Cells were grown as described by Berg and Turner (1993). They were tethered in motility medium with antipolyhook antibody, as described by Block et al. (1991), except that biotinylated protein A (Sigma, St. Louis, MO, 10 μ g/ml) was added 10 min after exposure of cells to antibody and the mixture was allowed to settle onto avidin-coated glass coverslips.

Received for publication 5 March 1996 and in final form April 26, 1996.

Address reprint requests to Dr. Howard Berg, Molecular and Cellular Biology, Harvard University, 16 Divinity Avenue, Cambridge, MA 02138. Tel: 617-495-0924; Fax: 617-496-1114; E-mail: hberg@biosun.harvard.edu.

© 1996 by the Biophysical Society

0006-3495/96/08/918/06 \$2.00

TABLE 1 Bacterial strains and plasmids used in this study

Strain	Relevant genotype/background	PI construction	Selection/screen	Source or reference
AW405	Wild-type for chemotaxis			Armstrong et al., 1967
RP5099	<i>eda50 zea::Tn10</i>			J. S. Parkinson
MS5037	<i>motA448</i>			M. I. Simon
JA11	$\Delta fliC::kan$			R. M. Macnab
HCB1254	$\Delta fliC::kan$ <i>motA448</i> pDFB36	JA11 \times MS5037	$Kn^R Ap^R$	This study
ADTS1	<i>eda50 zea::Tn10 motA448</i>	RP5099 \times MS5037	Tc^R/eda^-	This study
RP4979	<i>eda^+ \Delta m43-10(cheY)</i>			J. S. Parkinson
HCB1255	<i>eda^+ \Delta m43-10(cheY) motA448</i>	RP4979 \times ADTS1	<i>eda^+/Tc^S</i> , <i>che^-</i>	This study
HCB1256	<i>eda^+ \Delta m43-10(cheY) motA448</i> pDFB36		Ap^R	This study
HCB758	<i>pilA'-kan/AW405</i>			Fung, 1994
ADTS2	<i>eda^+ \Delta m43-10(cheY) motA448 pilA'-kan</i>	HCB758 \times HCB1255	Kn^R	This study
HCB1257	<i>fliC::Tn10</i>			Kuwajima, 1988
HCB8	<i>fliC* fliK694#</i> /AW405			Lab strain
ADTS3	<i>fliC::Tn10 fliK694</i>	HCB1257 \times HCB8	$Tc^R/fliK$	This study
HCB1258	<i>fliC::Tn10 fliK694 eda^+ \Delta m43-10(cheY)</i>	ADTS3 \times ADTS2	$Tc^R/fliK$	This study
	<i>motA448 pilA'-kan</i>			
HCB1259	<i>fliC::Tn10 fliK694 eda^+ \Delta m43-10(cheY)</i>		Ap^R	This study
	<i>motA448 pilA'-kan</i> pDFB36			
Plasmid pDFB36	<i>plac-motA^+, lacI^Q, Ap^R</i>			Blair and Berg, 1988

**fliC* from YK4161, gift of M. I. Simon.

#*fliK694* from YK4105, gift of M. I. Simon.

Strain HCB1259 (Table 1) lacks pili, produces polyhooks, and has motors that, when repaired, spin only counterclockwise. The strain was constructed as follows:

Step 1: ADTS1 was made by transducing *eda50 zea::Tn10-3* from RP5099 into MS5037.

Step 2: HCB1255 was made by transducing the deletion $\Delta m43-10(cheY)$ from RP4979 into ADTS1. Transductants were selected that had acquired the wild-type *eda* gene and lost the *Tn10* marker. HCB1256 was made by transforming HCB1255 with pDFB36. We confirmed the acquisition of the deletion $\Delta m43-10(cheY)$ and retention of the *motA448* allele by testing the phenotype of HCB1256. The motors of HCB1256 are paralyzed. In the presence of IPTG the cells produce wild-type MotA, and the motors are repaired.

Step 3: ADTS2 was made by transducing *pilA'-kan* from HCB758 into HCB1255.

Step 4: ADTS3 was made by transducing *fliC::Tn10* from HCB1257 into HCB8.

Step 4: HCB1258 was made by transducing the genes *fliC::Tn10* and *fliK694* from ADTS3 into ADTS2.

Step 5: HCB1259 was made by transforming HCB1258 with pDFB36.

In summary, HCB1259 has the following genotype (and phenotype): *motA448* (produces paralyzed motors), *pilA'-kan* (does not produce type 1 pili), $\Delta m43-10(cheY)$ (has motors that, when resurrected, spin only counterclockwise), *fliK694* and *fliC::Tn10* (produce polyhooks but no filaments), and contains pDFB36 (produces wild-type MotA when exposed to IPTG).

Cells were grown as described by Berg and Turner (1993) and tethered in motility medium with antipolyhook antibody as described by Block et al. (1991).

Data acquisition

We used a flow cell to allow exchange of media (Berg and Block, 1984). Cells were studied in 80% motility medium, 20% tryptone broth, and 2.5 mM IPTG. We monitored their rotation with a linear-graded filter apparatus (Berg and Turner, 1993), selecting cells that spun slowly and showed abrupt changes in rate, indicating gain or loss of torque-generating units.

Data analysis

First, we separated the data record for each motor into segments corresponding to distinct levels (by hand), skipping regions where the motor

switched back and forth between adjacent levels or was clearly subjected to external noise (as happens, for example, when a cell partially untethers part way through an experiment). Each segment represented at least 100 consecutive revolutions.

Second, we applied fluctuation analysis to each data segment. When a stepping motor travels a fixed angular distance θ it takes a fixed number of steps k . The variance in the time required to travel this distance and the mean time are related to k by the expression (e.g., Samuel and Berg (1995), Eq. 18):

$$k = \frac{\langle T \rangle^2}{\langle T^2 \rangle - \langle T \rangle^2}. \quad (1)$$

If N is the number of steps per revolution and n is the integral number of revolutions analyzed (in successive, nonoverlapping blocks), then $k = nN$. Also, the mean time to travel n revolutions, $\langle T_n \rangle$, is just $n\langle T_1 \rangle$, where $\langle T_1 \rangle$ is the mean rotation period for a single revolution. Therefore,

$$\langle T_n^2 \rangle - \langle T_n \rangle^2 = n \frac{\langle T_1^2 \rangle}{N}. \quad (2)$$

It follows that we can determine N from the slope of a plot of variance in rotation period as a function of the number of revolutions per period, n . Error in the regression fit of variance versus n leads to error in our estimate of N (Parratt, 1961). Equation 1 is strictly valid for a Poisson stepper. As noted above, if the waiting times for successive steps are not statistically independent or are not exponentially distributed, then N is an over estimate of the actual number of steps per revolution.

RESULTS

Data obtained for one cell of strain HCB1259, exhibiting three levels of torque, are shown in Fig. 1. Each level of torque for every motor studied appeared to be an integral multiple between 1 and 8 of a unitary torque (Fig. 2). Lines fitted to each set of rates had different slopes, because the cells were of different sizes and had different tethering geometries (had different viscous drag coefficients), but each line projected to the origin.

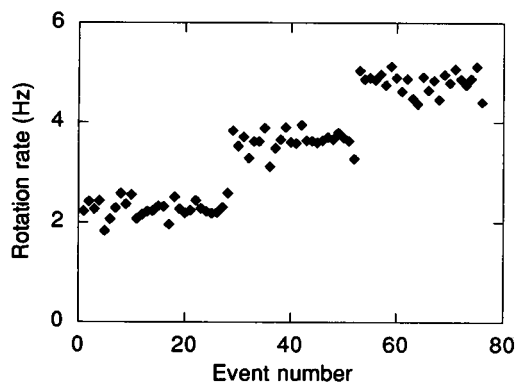


FIGURE 1 Resurrection of a single motor, showing discrete and abrupt changes in rotation rate, which indicate the acquisition of active torque-generating units. The mean rate is plotted for events that comprise four consecutive revolutions. The symbol used to denote a particular cell is the same in all figures.

For each cell we plotted the variance in period, $\langle T_n^2 \rangle - \langle T_n \rangle^2$, for different numbers of revolutions n , as shown in Fig. 3. These plots were highly linear, confirming that variance is due to motor stochasticity. As cells acquired torque-generating units, the slopes of the variance-versus- n plots decreased; their motors spun more smoothly, and the estimate of the number of steps per revolution increased (Fig. 4). This increase was approximately linear, as expected if each torque-generating unit steps independently.

In Fig. 5 we plot the estimate of the number of steps per revolution as a function of the estimate of the number of active torque-generating units. This plot is not affected by differences in viscous drag coefficients. However, it is affected by all extraneous sources of noise, including twisting or bending of the tether as the result of Brownian movement. This noise will only decrease the estimate of the number of steps per revolution. Therefore, the data corresponding to the uppermost points in Fig. 4 are probably least affected. A line can be drawn through these points that projects to the origin. Regression analysis (dashed curve)

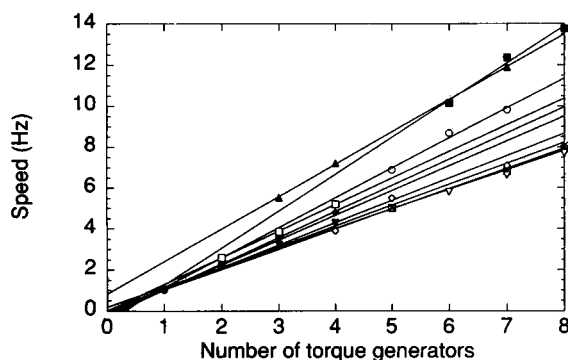


FIGURE 2 Mean speed at each discrete level of torque, plotted as a function of the number of torque-generating units deemed active at that level, for all the cells used in this study. A regression line is drawn for each cell. (●) denotes a cell of strain HCB1254. All other symbols denote cells of strain HCB1259.

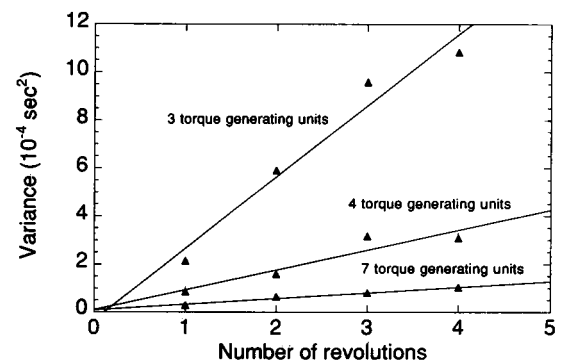


FIGURE 3 Variance in rotation period for n revolutions versus n for one cell. The three different lines are computed for three different data segments distinguished by the number of active torque-generating units shown.

also indicates approximate linearity. Thus, our results support the proposition that the number of steps per revolution, estimated from Eq. 2, is proportional to the number of torque-generating units.

DISCUSSION

Theoretical models of the flagellar motor can be categorized into those with stepping drives that move discontinuously and those with fluid drives that do not. A brief review of most of the models that have been proposed is given elsewhere (Berg and Turner, 1993). Stepping drives prohibit free motion between the rotor and the stator: long-term variability in rotation rate derives solely from the variability in intervals between steps. Fluid drives also exhibit long-term drift that is due to Brownian movement.

Existing evidence argues against a fluid drive. First, treatment with 2,4-dinitrophenol, an uncoupler of oxidative phosphorylation, arrests rotation. Motors of treated cells eventually lock up and resist externally applied torque (Berg, 1976; Block et al., 1989). Second, when motors are driven backward by an externally applied torque that barely

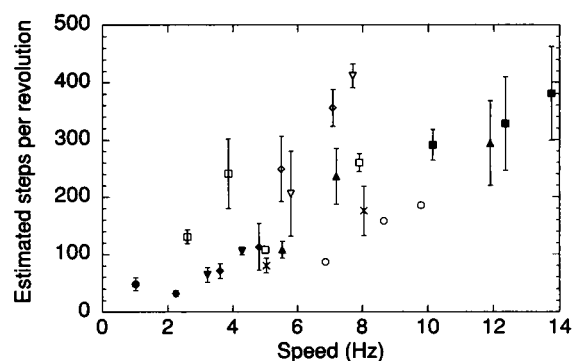


FIGURE 4 Estimated number of steps per revolution plotted as a function of the mean rotation rate at each discrete level of torque for every cell. See Materials and Methods for the method for calculation of the estimate and of the error bars.

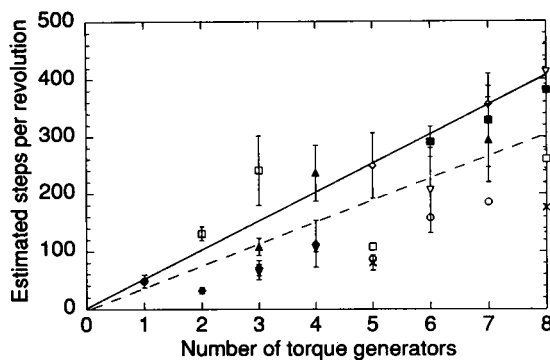


FIGURE 5 Step-number estimate from Fig. 4, plotted as a function of the torque level estimate of Fig. 2, for every cell. The solid line was drawn by hand through the uppermost points; see the text. The dashed line was obtained by linear regression ($r = 0.74$).

exceeds the motor torque, they creep steadily, as slowly as one revolution in 12 min (the slowest cell clocked by Berg and Turner, 1993). But a tethered cell is hydrodynamically equivalent to a sphere with a radius of $\sim 1 \mu\text{m}$; if it were free to rotate, it would move erratically, with Brownian motion carrying it through a root-mean-square angle of 2π (one revolution) in ~ 2 min. Third, if fluctuations in rotation rate were due simply to diffusion, then the variance in rotation period should decrease inversely as the cube of the mean rotation rate, as observed for tethered cells with broken motors; however, intact motors produce an inverse square dependence (Samuel and Berg, 1995).

Naively, one might expect motion of a tethered cell driven by a stepping motor to be discontinuous. Why are steps not apparent? The main problem is elasticity in the tether. If the motor generates a torque M , the tether twists through an angle M/B , where B is its torsional spring constant. When the motor stops generating torque, the tether unwinds, continuing to drive the cell body forward. Consequently, the amplitudes of discontinuities in the motion of the cell body are much smaller than those in the driving torque. In a motor with sinusoidal angular flutter analyzed earlier (Berg, 1976), elasticity in the tether decreased the amplitude of the flutter in the cell body by a factor of $1/(1 + N^2\theta_0^2)^{1/2}$, where N is the number of steps per revolution and θ_0 is the mean twist of the tether. This twist is equal to the product of the mean angular velocity of the cell and the time constant for exponential decay in the twist, observed when the tether is clamped to the cell body. If the rotor suddenly moves relative to the stator a fixed angular distance, ϕ , the tether is wound up by an angle ϕ . The torque exerted by the tether on the cell body increases by an amount $B\phi$, and then it decreases exponentially as the cell body rotates, allowing the tether to unwind. The initial displacement of the rotor is not apparent in the displacement of the cell body until one waits for this decay. Unfortunately, the mean twist in the tether can be large (more than 2π rad) and the decay constant can be long (a few tenths of a second; cf. Block et al., 1989, 1991). So the rotation of the cell body is much smoother than that of the motor.

There are several ways in which things might be improved: 1) Reduce the time constant for the exponential decay by increasing the stiffness of the tether. This is not easy, because most of the compliance appears to be in the hook rather than in the filament (Block et al., 1991). 2) Reduce the time constant for the exponential decay by reducing the load on the motor, either by tethering minicells or by looking at free rotation of hooks. This introduces technical difficulties, because the rotation rate for an unloaded motor can be several hundred hertz (Berg and Turner, 1993). 3) Reduce motor speed, so that the interval between steps is long compared with the time constant for exponential decay. This might be done by using cells with only one torque-generating unit or by working at a lower temperature or at a reduced protonmotive force. One also might apply external torque and drive cells slowly backward.

In theoretical stepping drives, each step is the result of a reaction cycle comprising several sequential processes. The waiting time between steps is the duration of the reaction cycle. Inasmuch as each constitutive sequential process of the cycle is stochastic, the duration of the cycle also is stochastic. In general, cycle duration is drawn from a probability distribution that is the convolution of the probability distributions of the waiting time for each constitutive reaction (Schnitzer and Block, 1996). But, if the cycle is dominated by one rate-limiting process, then cycle durations will be exponentially distributed, as in the Poisson stepper. We estimated the number of steps per revolution, as described in Materials and Methods. For the Poisson stepper, this calculation gives the actual number of steps per revolution. For non-Poisson steppers, this calculation is simply proportional to the actual number of steps per revolution. Whether the flagellar motor is Poisson or not, it generates the same fluctuations in rotation rate as a Poisson stepper that takes at least 400 steps per revolution. Also, the calculated number of steps per revolution, and therefore the actual number of steps per revolution, is proportional to the number of active torque-generating units. A successful theoretical model for the flagellar motor should exhibit both of these properties.

A set of distinct torque-generating units drives the motor. Through resurrection studies, Block and Berg (1984) argued for 16 units, whereas Blair and Berg (1988) found evidence for at most 8. Reactivation following de-energization was consistent with 8 (Fung and Berg, 1995), whereas studies of mechanical breakage and repair suggested as many as 11 (Berry et al., 1995). Although we could comfortably assign values between 1 and 8 to any level of torque, we could just as easily have assigned values between 2 and 16, provided that sudden jumps occurred by two levels instead of one. This would not change our basic conclusions, namely, that wild-type motors step at least 400 times per revolution and that individual torque-generating units step independently.

We have shown that, as the motor acquires torque-generating units, it takes more steps per revolution. But this implies that the size of each step must decrease. Presum-

ably, each torque-generating unit steps along the same set of binding sites at the periphery of the rotor, whose separation does not depend on the number of units that happen to be active. This apparent contradiction is reconcilable if each torque-generating unit is linked to the rigid framework of the cell wall by a spring. Consider such a motor with a single torque-generating unit. Suppose that this unit suddenly steps a distance d from one binding site to the next. Provided that its spring is much less compliant than the tether linking the rotor to the glass coverslip, this unit will pull the rotor back a distance d and thus will wind the tether through an angle of approximately d/r , where r is the radius of the ring of binding sites. If this movement could be discerned, the apparent step size would be the same as the separation between binding sites. But what if two torque-generating units are active? In this case, if one unit steps a distance d , it will pull the rotor back only a distance $d/2$, because it must also stretch the spring of the second-torque generating unit, which has the same compliance as that of the first. Similarly, if there are three units, the rotor will move a distance $d/3$, and so on. Thus, as the motor acquires torque-generating units (units that step independently), it will take more steps per revolution, and the step size will decrease.

According to this analysis, there should be at least 50 binding sites at the periphery of the rotor. Current estimates of the stoichiometry of the MS-ring protein, FliF, and by inference, of the protein thought to interact with the torque-generating units, FliG, are ~ 26 subunits (Jones et al., 1990; Sosinsky et al. 1992; Francis et al., 1992; Lloyd et al., 1996). So there should be at least two binding sites per subunit. Assuming that these sites are located at a diameter of ~ 25 nm (Francis et al., 1994; Katayama et al., 1996) their spacing is at most 1.5 nm. For a recent review of flagellar motor structure, see Macnab (1996).

Leibler and Huse (1993) constructed a generalized theory of molecular motors that unifies "porters" (stochastic stepers that prohibit free motion) and "rowers" (models that allow free motion). Although Leibler and Huse had eukaryotic motors in mind, their theory is applicable to stochastic stepping models and fluid drive mechanisms for the bacterial flagellar motor. By locating the bacterial flagellar motor as a "porter" within the scheme of Leibler and Huse, the present study justifies comparison of flagellar motors with eukaryotic "porters," e.g., kinesin. As much as the flagellar motor and their eukaryotic counterparts pose different challenges, they also afford different opportunities. Individual kinesin steps have been seen directly (Svoboda et al., 1993; Coppin et al., 1996). On the other hand, ensembles of known numbers of stepping elements in the flagellar motor are much easier to prepare and study than ensembles of kinesin.

Kara-Ivanov et al. (1995) considered the contribution of association and dissociation of torque-generating units to fluctuations observed in the rotation rate of tethered cells. The rate constants deduced for these processes were of the order of 1 s^{-1} . However, resurrecting motors do not exhibit

such rapid kinetics (Fig. 1). The fluctuations examined in our study are the result of stepping stochastics, not of acquisition and loss of torque-generating units.

We thank Karen Fahrner for guidance and Patrick Murphy for assistance in the construction of HCB1254 and HCB1259. We also thank Steve Block, Mark Schnitzer, Alan Stern, Richard Berry, and Linda Turner for comments on the manuscript and Karel Svoboda for inspiring discussions. A.D.T.S. received a stipend from a Molecular Biophysics Training grant from the National Institutes of Health. This research was supported by grant MCB-9213011 from the National Science Foundation and by the Rowland Institute for Science.

REFERENCES

- Berg, H. C. 1976. Does the flagellar rotary motor step? *In* Cell Motility, Vol. 3. R. Goldman, T. Pollard, and J. Rosenbaum, editors. Cold Spring Harbor Laboratories, Cold Spring Harbor, NY. 47–56.
- Berg, H. C., and R. A. Anderson. 1973. Bacteria swim by rotating their flagellar filaments. *Nature (London)*. 245:380–382.
- Berg, H. C., and S. M. Block. 1984. A miniature flow cell designed for rapid exchange of media under high-power microscope objectives. *J. Gen. Microbiol.* 130:2915–2920.
- Berg, H. C., M. D. Manson, and M. P. Conley. 1982. Dynamics and energetics of flagellar rotation in bacteria. *Soc. Exp. Biol. Symp.* 35: 1–31.
- Berg, H. C., and L. Turner. 1993. Torque generated by the flagellar motor of *Escherichia coli*. *Biophys. J.* 65:2201–2216.
- Berry, R. M., L. Turner, and H. C. Berg. 1995. Mechanical limits of bacterial flagellar motors probed by electrorotation. *Biophys. J.* 69: 280–286.
- Blair, D. F., and H. C. Berg. 1988. Restoration of torque in defective flagellar motors. *Science*. 242:1678–1681.
- Block, S. M., and H. C. Berg. 1984. Successive incorporation of force-generating units in the bacterial rotary motor. *Nature (London)*. 309: 470–472.
- Block, S. M., D. F. Blair, and H. C. Berg. 1989. Compliance of bacterial flagella measured with optical tweezers. *Nature (London)*. 338: 514–517.
- Block, S. M., D. F. Blair, and H. C. Berg. 1991. Compliance of bacterial polyhooks measured with optical tweezers. *Cytometry*. 12:492–496.
- Coppin, C. M., J. T. Finer, J. A. Spudis, and R. D. Vale. 1996. Detection of sub-8-nm movements of kinesin by high-resolution optical-trap microscopy. *Proc. Natl. Acad. Sci. USA*. 93:1913–1917.
- Francis, N. R., V. M. Irikura, S. Yamaguchi, D. J. DeRosier, and R. M. Macnab. 1992. Localization of the *Salmonella typhimurium* flagellar switch protein FliG to the cytoplasmic M-ring face of the basal body. *Proc. Natl. Acad. Sci. USA*. 89:6304–6308.
- Francis, N. R., G. E. Sosinsky, D. Thomas, and D. J. DeRosier. 1994. Isolation, characterization and structure of bacterial flagellar motors containing the switch complex. *J. Mol. Biol.* 235:1261–1270.
- Fung, D. C. Y. K. 1994. Powering the *Escherichia coli* flagellar motor with an external voltage source. Ph.D thesis. Harvard University, Cambridge, MA. 117 pp.
- Fung, D. C., and H. C. Berg. 1995. Powering the flagellar motor of *Escherichia coli* with an external voltage source. *Nature (London)*. 375:809–812.
- Jones, C. J., R. M. Macnab, H. Okino, and S.-I. Aizawa. 1990. Stoichiometric analysis of the flagellar hook-(basal-body) complex of *Salmonella typhimurium*. *J. Mol. Biol.* 212:377–387.
- Kara-Ivanov, M., M. Eisenbach, and S. R. Caplan. 1995. Fluctuations in rotation rate of the flagellar motor of *Escherichia coli*. *Biophys. J.* 69:250–263.
- Katayama, E., T. Shiraishi, K. Oosawa, N. Baba, and S.-I. Aizawa. 1996. Geometry of the flagellar motor in the cytoplasmic membrane of *Salmonella typhimurium* as determined by stereo-photogrammetry of quick-freeze deep-etch replica images. *J. Mol. Biol.* 255:458–475.

- Kuwajima, G. 1988. Flagellin domain that affects H antigenicity of *Escherichia coli* K-12. *J. Bacteriol.* 170:485–488.
- Leibler, S., and D. A. Huse. 1993. Porters versus rowers: a unified stochastic model of motor proteins. *J. Cell. Biol.* 121:1357–1368.
- Lloyd, S. A., H. Tang, X. Wang, S. Billings, and D. F. Blair. 1996. Torque generation in the flagellar motor of *Escherichia coli*: evidence of a direct role for FliG but not for FliM or FliN. *J. Bacteriol.* 178:223–231.
- Macnab, R. M. 1996. Flagella and motility. In *Escherichia coli* and *Salmonella*: Cellular and Molecular Biology, 2nd ed. F. C. Neidhardt, editors. American Society for Microbiology, Washington, D.C. 123–145.
- Parratt, L. G. 1961. Probability and Experimental Errors in Science. Dover, New York. 109–135.
- Samuel, A. D. T., and H. C. Berg. 1995. Fluctuation analysis of rotational speeds of the bacterial flagellar motor. *Proc. Natl. Acad. Sci. USA.* 92:3502–3506.
- Schnitzer, M. J., and S. M. Block. 1996. Statistical kinetics of processive enzymes. *Cold Spring Harbor Symp. Quant. Biol.* 60:793–802.
- Silverman, M., and M. Simon. 1974. Flagellar rotation and the mechanism of bacterial motility. *Nature (London).* 249:73–74.
- Sosinsky, G. E., N. R. Francis, D. J. DeRosier, J. S. Wall, M. N. Simon, and J. Hainfield. 1992. Mass determination and estimation of subunit stoichiometry of the bacterial hook-basal body flagellar complex of *Salmonella typhimurium* by scanning transmission electron microscopy. *Proc. Natl. Acad. Sci. USA.* 89:4801–4805.
- Svoboda, K., P. P. Mitra, and S. M. Block. 1994. Fluctuation analysis of motor protein movement and single enzyme kinetics. *Proc. Natl. Acad. Sci. USA.* 91:11782–11786.
- Svoboda, K., C. F. Schmidt, B. J. Schnapp, and S. M. Block. 1993. Direct observation of kinesin stepping by optical trapping interferometry. *Nature (London).* 365:721–727.